

# Q-switched ytterbium doped fiber laser using multi-walled carbon nanotubes saturable absorber

N. Kasim<sup>1</sup>, A. H. H. Al-Masoodi<sup>2</sup>, F. Ahmad<sup>3</sup>, Y. Munajat<sup>1</sup>, H. Ahmad<sup>2</sup>, and S. W. Harun<sup>1,2,3\*</sup>

<sup>1</sup>Advanced Photonics Science Institute, Faculty of Science, University Technology Malaysia, 81310 Skudai, Johor, Malaysia

<sup>2</sup>Photonics Research Centre, University of Malaya, 50603 Kuala Lumpur, Malaysia

<sup>3</sup>Department of Electrical Engineering, Faculty of Engineering, University of Malaya, 50603, Kuala Lumpur, Malaysia

\*Corresponding author: swharun@um.edu.my

Received December 12, 2013; accepted January 22, 2014; posted online February 28, 2014

A Q-switched ytterbium-doped fiber laser (YDFL) is proposed and demonstrated using a newly developed multi-walled carbon nanotubes polyethylene oxide (MWCNTs-PEO) film as a passive saturable absorber (SA). The saturable absorber is prepared by mixing the MWCNTs homogeneous solution into a dilute PEO polymer solution before it is left to dry at room temperature to produce thin film. Then the film is sandwiched between two FC/PC fiber connectors and integrated into the laser cavity for Q-switching pulse generation. The laser generates a stable pulse operating at wavelength of 1060.2 nm with a threshold pump power of 53.43 mW. The YDFL generates a stable pulse train with repetition rates ranging from 7.92 to 24.27 kHz by varying 980-nm pump power from 53.42 to 65.72 mW. At 59.55-mW pump power, the lowest pulse width and the highest pulse energy are obtained at 12.18  $\mu$ s and 143.5 nJ, respectively.

OCIS codes: 140.0140, 060.0060, 190.0190

doi: 10.3788/COL201311.031403.

Highly stable and compact pulsed ytterbium-doped fiber lasers (YDFLs) are very attractive because of their compactness, flexibility, and low cost<sup>[1–6]</sup>. They have been found in a vast range of applications in recent years including optical imaging, fiber communications, and material processing. A short optical pulse operating in microsecond and nanosecond regions can be realized by sudden switching of the cavity Q factor or the cavity loss. Active Q-switching is typically achieved by inserting an acoustic-optic or an electro-optic modulator into the cavity<sup>[7]</sup>. On the other hand, passive Q-switching by means of saturable absorbers (SAs) is a convenient technique to simplify the cavity design and eliminate the need for external Q-switching electronics. Semiconductor saturable absorber mirrors (SESAMs)<sup>[8]</sup>, and carbon nanotubes (CNTs)<sup>[9]</sup> are normally used as the SA for the Q-switched YDFLs. However, the fabrication of SESAMs requires very complex and costly processes. Furthermore, they are not compatible with optical fiber, which limits their widespread application. The newly-developed single-walled carbon nanotubes saturable absorbers (SWCNT-SAs) have the remarkable features of fiber compatibility, easy fabrication, and low cost over the traditional SAs<sup>[10,11]</sup>, along with the advantage of wide operating bandwidth.

Recently, a new member of carbon nanotubes family, multi-walled carbon nanotubes (MWCNTs)<sup>[12,13]</sup> have also attracted many attentions because they possess many advantages in nonlinear optics. The growth of the MWCNT material does not need complicated techniques or special growing conditions so that its production yield is high for each growth. Therefore the production cost of MWCNT material is reasonably lower than that of SWCNT material<sup>[14]</sup>. Additionally, MWCNT material has good thermal characteristics, which is of great importance for high power ultrafast laser development. Compared with SWCNTs, the MWCNTs also have higher

mechanical strength, better thermal stability as well as can absorb more photons per nanotube due to its higher mass density of the multi-walls. These favorable features are due to the structure of MWCNTs which takes the form of a stack of concentrically rolled graphene sheets. The outer walls can protect the inner walls from damage or oxidation so that the thermal or laser damage threshold of MWCNT is higher than that of the SWCNTs<sup>[15]</sup>.

To date, there are only a few reported works on application of MWCNTs material as a saturable absorber<sup>[16]</sup>. In this letter, a Q-switched YDFL is demonstrated using a new developed MWCNTs-SA. The SA is constructed by sandwiching a MWCNTs- polyethylene oxide (MWCNTs-PEO) film between two fiber connectors. The laser delivered Q-switched pulses with the repetition rate in a range from 7.92 to 24.27 kHz with the maximum pulsed energy of 143.5 nJ.

The MWCNTs material used for the fabrication of the absorber in this experiment is functionalized so that it can be dissolved in water. The diameter of the MWCNTs used is about 10–20 nm and the length distribution is from 1 to 2  $\mu$ m. The functionalizer solution was prepared by dissolving 4 g of sodium dodecyl sulphate (SDS) in 400-ml deionized water. 250-mg MWCNT was added to the solution and the homogenous dispersion of MWCNTs was achieved after the mixed solution was sonicated for 60 minutes at 50 W. The solution was then centrifuged at 1000 rpm to remove large particles of undispersed MWCNTs to obtain a stable dispersed suspension. MWCNTs-PEO composite was prepared by adding the dispersed MWCNTs suspension into a PEO solution by one to one ratio. PEO solution was prepared by dissolving 1 g of PEO ( $M_w=1\times 10^6$  g/mol) in 120 ml of deionized water. The homogeneous MWCNTs-PEO composite was obtained by sonification process for more than 1 hour. The CNT-PEO composite was casted onto a glass petri dish and left to dry at room temperature

for about one week to produce thin film with thickness around  $10\ \mu\text{m}$ .

Figure 1 shows the Raman spectrum of the MWCNTs film when it is excited by a 532-nm laser. It is shown that the Raman spectrum bears a lot of similarity to graphene, which is not too surprising as the MWCNT has many layers of graphene wrapped around the core tube. We can see well defined G ( $1580\ \text{cm}^{-1}$ ) and G' ( $2705\ \text{cm}^{-1}$ ) bands as there were in graphene and graphite. The G band originates from in-plane tangential stretching of the carbon-carbon bonds in graphene sheet. We also see a prominent band around  $1350\ \text{cm}^{-1}$ , which is known as the D band. This indicates that the carbon nanotubes type is multi-walled, which has multi-layer configuration and disorder structure. The D band originates from a hybridized vibrational mode associated with graphene edges and it indicates the presence of some disorder to the graphene structure. As expected, the radial breathing mode (RBM) bands, which correspond to the expansion and contraction of the tubes, are not present in the MWCNT because the outer tubes restrict the breathing mode. The D' band which is a weak shoulder of the G-band is also observed at  $1608\ \text{cm}^{-1}$  due to double resonance feature induced by disorder and defect. In addition, others distinguishable features like D + G band ( $2880\ \text{cm}^{-1}$ ), a small peak at  $839\ \text{cm}^{-1}$  and Si were also observed as depicted in Fig. 1.

The experimental setup of the proposed *Q*-switched YDFL is shown in Fig. 2, which consists of a 2-m-long ytterbium-doped fiber (YDF), a 980/1050-nm wavelength division multiplexer (WDM), a MWCNTs-PEO film based SA, optical isolator, and 3-dB output coupler in a ring configuration. The saturable absorber is fabricated by cutting a small part of the earlier prepared film ( $2\times 2\ \text{mm}^2$ ) and sandwiching it between two FC/PC fiber connectors, after depositing index-matching gel onto the fiber ends. The insertion loss of the SA is measured to be around 2 dB at 1050 nm. The YDF used has a core diameter of  $4.0\ \mu\text{m}$ , (numerical aperture) NA of 0.20 and cutoff wavelength of around 980 nm. The doping levels of erbium and ytterbium ions in the fiber are 1000 and 1500 ppm, respectively. The YDF is pumped by a 980-nm laser diode via the WDM. Isolator is located between coupler and the SA to ensure unidirectional propagation of oscillating laser. The output of the laser is tapped

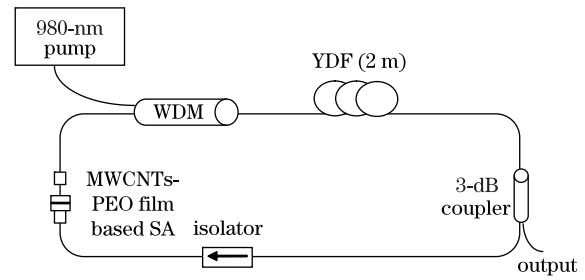


Fig. 2. Configuration of the proposed *Q*-switched YDFL utilizing a MWCNTs-PEO film based SA.

out of the cavity through a 3-dB coupler. The optical spectrum analyser (OSA, Yokogawa, AQ6370B) is used for the spectral analysis of the *Q*-switched YDFL with a spectral resolution of  $0.02\ \text{nm}$  whereas the oscilloscope (OSC, Tektronix, TDS 3052C) is used to observe the output pulse train of the *Q*-switched operation via a 460-kHz bandwidth photo-detector (Thor lab, PDA50B-EC). The total cavity length of the ring resonator is measured to be around 12 m.

In the experiment, the YDFL started to generate a self-starting *Q*-switching pulse at threshold pump power of 53.42 mW. When the pump power was gradually increased from 53.42 to 65.72 mW, the stable pulse trains with the different repetition rates were observed. It is also observed that further increase of the pump power results in unstable pulsation. Figure 3 shows the output spectrum of the YDFL when the pump is fixed at 53.42 mW. As seen, the YDFL operates at 1060.2 nm with signal-to-noise ratio (SNR) of around 23 dB. Some interference structures are also observed in the spectrum, which is most probably due to a nonlinear polarisation rotation effect in the ring cavity. Figure 4 shows the oscilloscope trace of the *Q*-switched pulse trains and its typical pulse envelope at three different pumping powers of 53.42, 59.55, and 65.72. The pulse trains show the typical feature of passive *Q*-switching and no timing jitter is noticeable (limited by the sensitivity of 460-kHz detector). The pulse train has the periods of 126, 75, and  $41\ \mu\text{s}$ , which corresponds to repetition rates of 7.92, 13.31, and 24.27 kHz at pump powers of 53.42, 59.55, and 65.72 mW, respectively. The corresponding pulse envelope has the the symmetrical Gaussian-like shape with full-width at half-maximum (FWHM) of 13.56, 12.18, and  $16.2\ \mu\text{s}$ , respectively.

Figure 5 shows the repetition rate and average output power as a function of 980-nm pump power. It is found that both repetition rate and average output power

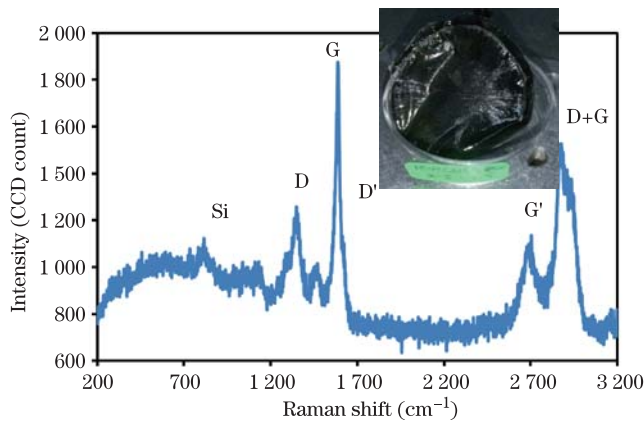


Fig. 1. Raman spectroscopy of MWNTs-PEO composites thin film. Inset: MWNTs-PEO thin film.

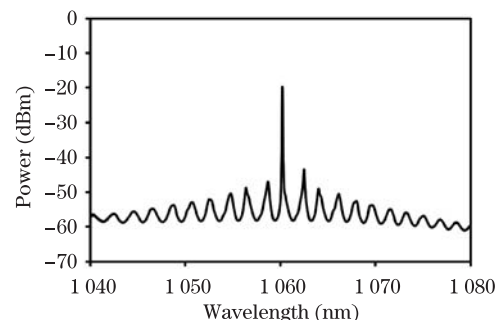


Fig. 3. Output spectrum of the proposed *Q*-switched YDFL at the threshold pump power of 53.42 mW.

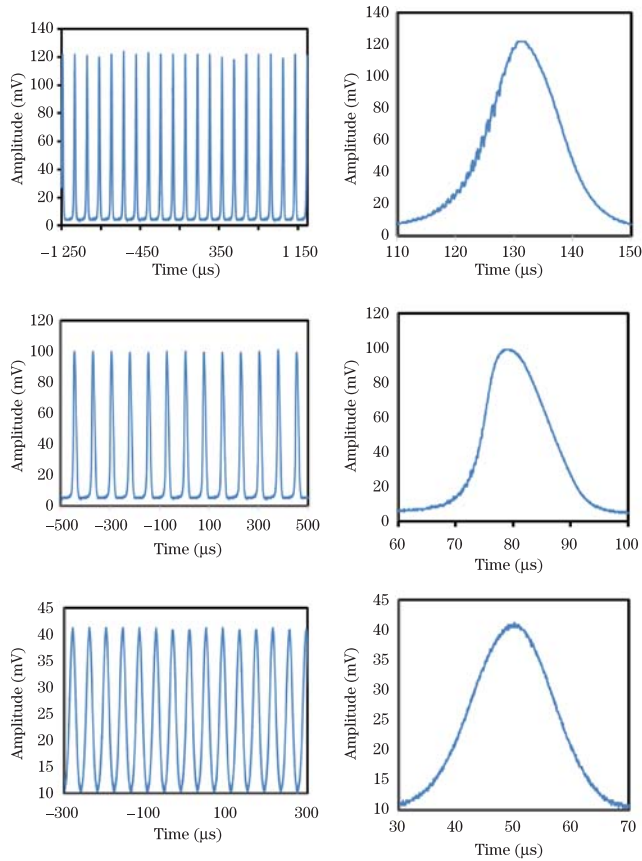


Fig. 4. *Q*-switched YDF of pulse train and single-pulse envelop at 980-nm pump powers of (a) 53.43 mW (repetition rate of 7.92 kHz), (b) 59.55 mW (repetition rate of 13.31 kHz), and (c) 65.72 mW (repetition rate of 24.27 kHz).

monotonically increases with the pump power. The repetition rate is detuned from 7.92 to 24.27 kHz as the pump power increases from 53.43 to 65.72 mW, further confirming the constructed laser is working under passive *Q*-switching. Unlike passively mode-locking condition where the repetition rate of the output pulses is fixed corresponding to the cavity length<sup>[17]</sup>, the repetition rate of a *Q*-switched fiber laser can be varied with reference to the lifetime of gain medium as well as pump power. Since different pump powers induce different time required to replenish the extracted energy between two consecutive pulses, the detuning of repetition rate takes place. A stable *Q*-switching can be maintained up to a pump power of 65.72 mW, where we obtain the maximum output power of 3.47 mW and repetition rate of 24.27 kHz.

It is found that the average output power increases from 0.68 to 3.47 mW as the pump power is increased from 53.43 to 65.72 mW. This is attributed to the Yb ions in the gain medium, which are excited to higher level even faster and the carbon nanotubes are saturated faster as well which gives higher repetition rate and shorter pulses<sup>[18]</sup>. In the experiment, when more gain is provided to saturate the SA, pulse energy is found to grow monotonically with the increment of the pump power from 53.43 to 59.55 mW as shown in Fig. 6. The pulse energy is unchanged with further increase of the pump power. This is due to the pulse width of output laser that exhibit the increment trend at this pump

power region. The YDFL operates at the maximum pulse energy of 143.5 nJ at pump power within 59.55 to 65.72 mW. It shows a stable operation without significant degradation of the deposited MWCNTs with such output pulse energy level. The pulse energy could be improved by reducing the insertion loss of the saturable absorber or by optimizing the laser cavity. On the other hand, the pulse width varies from 12.18 to 16.2 μs within the pump power range from 53.43 to 65.72 mW. However, the shortest pulse was emitting at the intermediate pump power of 59.55 mW. As the pump power increases, the non-radiative decay rate of Yb<sup>3+</sup> ions also increases. This generates heat in the laser cavity system where the MWCNTs ends up absorbing the accumulated heat. This will energize some electrons in the MWCNT's valence band to move up to the conduction band from the strong internal thermal motion. As less electron in the valence band are available for photon absorption, the initial transmittance of the SA becomes greater as the pump power or absorbed heat increases. Thus MWCNT's efficiency as saturable absorber is greatly reduced such that the pulse width begins to increase again after the saturation of SA as shown in Fig. 6. The *Q*-switching can be maintained up to a pump power of 65.72 mW, where the energy is larger than previously reported SWCNT based *Q*-switched fiber lasers<sup>[19]</sup>. The pulse becomes unstable and disappear as the pump power is further increased.

In conclusion, the ring configuration of the passively *Q*-switched YDFL is presented by using MWCNTs/PEO thin film as saturable absorber. The SA film is prepared

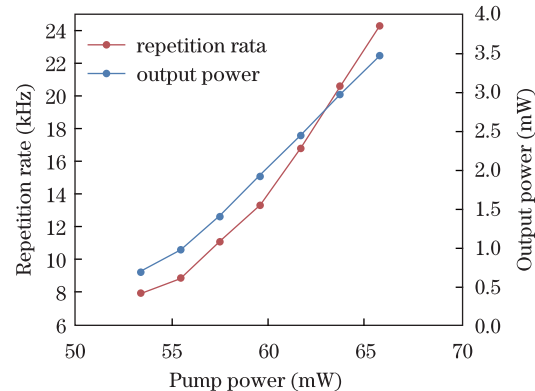


Fig. 5. Repetition rate and output power as a function of 980 nm of pump power.

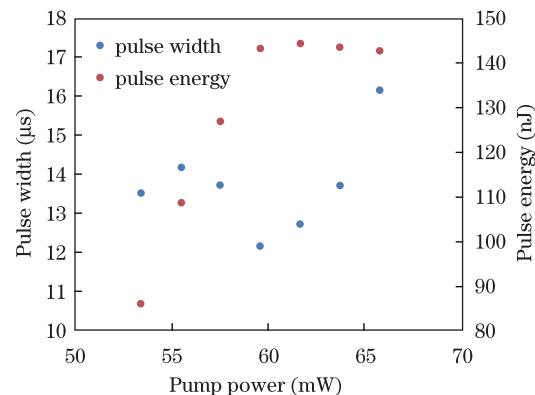


Fig. 6. Pulse width and pulse energy as a function of 980 nm of pump power.

by mixing the MWCNTs homogeneous solution into a dilute PEO polymer solution. It is sandwiched between two FC/PC fiber connectors and integrated into the laser cavity to generate a stable  $Q$ -switching pulse operating at wavelength of 1060.2 nm within pump power range from 53.43 to 65.72 mW. The repetition rate of the laser can be varied from 7.92 to 24.27 kHz by varying the pump power. At the 59.55-mW pump power, the lowest pulse width and the highest pulse energy are obtained at 12.18  $\mu$ s and 143.5 nJ, respectively.

This work was supported by Ministry of Higher Education under ERGS Grant scheme No. ER012-2012A.

## References

1. J. A. Alvarez-Chavez, H. L. Offerhaus, J. Nilson, P. W. Turner, W. A. Clarkson, and D. J. Richardson, *Opt. Lett.* **25**, 37 (2000).
2. Y. X. Fan, F. Y. Lu, S. L. Hu, K. C. Lu, H. J. Wang, X. Y. Dong, J. L. He, and H. T. Wang, *Opt. Lett.* **29**, 724 (2004).
3. Y. Wang and C. Q. Xu, *Appl. Opt.* **45**, 2058 (2006).
4. R. Zhu, J. Wang, J. Zhou, J. Liu, and W. Chen, *Chin. Opt. Lett.* **10**, 091402 (2012).
5. C. Zhou, Y. Liu, R. Zhu, S. Du, X. Hou, and W. Chen, *Chin. Opt. Lett.* **11**, 081403 (2013).
6. J. Yang, Y. Tang, J. Xu, *Photon. Res.* **1**, 52 (2013).
7. J. Jabczynski, W. Zendzian, and J. Kwiatkowski, *Opt. Express* **14**, 2184 (2006).
8. X. Yin, J. Meng, J. Zu, and W. Chen, *Chin. Opt. Lett.* **11**, 081402 (2013).
9. J. Lee, J. Koo, Y. M. Chang, P. Debnath, Y. W. Song, and J. H. Lee, *J. Opt. Soc. Am. B* **29**, 1479 (2012).
10. M. A. Ismail, S. W. Harun, N. R. Zulkepely, R. M. Nor, F. Ahmad, and H. Ahmad, *Appl. Opt.* **51**, 8621 (2012).
11. Z. Yu, Y. Song, C. Tian, J. Li, X. Zhang, and Y. Wang, in *Proceedings of the SPIE High-Power Lasers and Applications VI* 855115 (2012).
12. S. Iijima, *Nature* **354**, 56 (1991).
13. S. L. Su, Y. G. Wang, J. Liu, L. H. Zheng, L. B. Su, and J. Xu, *Laser Phys. Lett.* **9**, 120 (2012).
14. L. Zhang, Y. G. Wang, H. J. Yu, L. Sun, W. Hou, X. C. Lin, and J. M. Li, *Laser Phys.* **21**, 1382 (2011).
15. K. Ramadurai, C. L. Cromer, L. A. Lewis, K. E. Hurst, A. C. Dillon, R. L. Mahajan, and J. H. Lehman, *J. Appl. Phys.* **103**, 013103 (2008).
16. X. C. Lin, L. Zhang, Y. H. Tsang, Y. G. Wang, H. J. Yu, S. L. Yan, W. Sun, Y. Y. Yang, Z. Han, and W. Hou, *Laser Phys. Lett.* **10**, 055805 (2013).
17. S. W. Harun, R. Akbari, and H. Arof, H. Ahmad, *Laser Phys. Lett.* **8**, 449 (2011).
18. D. P. Zhou, L. Wei, B. Dong, and W. K. Liu, *IEEE Photon. Technol. Lett.* **22**, 9 (2010).
19. Z. Luo, Y. Huang, J. Weng, H. Cheng, Z. Lin, B. Xu, Z. Cai, and H. Xu, *Opt. Express* **21**, 29516 (2013).